Iron-dependent nitrogen cycling in a ferruginous lake and the nutrient status of Proterozoic oceans

Céline C. Michiels[1], François Darchambeau[2], Fleur A. E. Roland[2], Cédric Morana[3], Marc Llirós[4,5], Tamara García-Armisen[6], Bo Thamdrup[7], Alberto V. Borges[2], Donald E. Canfield[7], Pierre Servais[6], Jean-Pierre Descy[8] and Sean A. Crowe[1]*

Nitrogen limitation during the Proterozoic has been inferred from the great expanse of ocean anoxia under low-O_2 atmospheres, which could have promoted NO_3^- reduction to N_2 and fixed N loss from the ocean. The deep oceans were Fe rich (ferruginous) during much of this time, yet the dynamics of N cycling under such conditions remain entirely conceptual, as analogue environments are rare today. Here we use incubation experiments to show that a modern ferruginous basin, Kabuno Bay in East Africa, supports high rates of NO_3^- reduction. Although 60% of this NO_3^- is reduced to N_2 through canonical denitrification, a large fraction (40%) is reduced to NH_4^+, leading to N retention rather than loss. We also find that NO_3^- reduction is Fe dependent, demonstrating that such reactions occur in natural ferruginous water columns. Numerical modelling of ferruginous upwelling systems, informed by our results from Kabuno Bay, demonstrates that NO_3^- reduction to NH_4^+ could have enhanced biological production, fuelling sulfate reduction and the development of mid-water euxinia overlying ferruginous deep oceans. This NO_3^- reduction to NH_4^+ could also have partly offset a negative feedback on biological production that accompanies oxygenation of the surface ocean. Our results indicate that N loss in ferruginous upwelling systems may not have kept pace with global N fixation at marine phosphorous concentrations (0.04–0.13 μM) indicated by the rock record. We therefore suggest that global marine biological production under ferruginous ocean conditions in the Proterozoic eon may thus have been P not N limited.

As an element essential to life, nitrogen (N) often limits biological production[1]. N is made available to life through microbial fixation of atmospheric N_2. This N is liberated as NH_4^+ from decaying biomass, and oxidized to NO_3^- in the presence of oxygen. N is returned to the atmosphere through NO_3^- reduction to N_2 under low O_2 conditions. Two microbial processes are responsible for N_2 production; denitrification, which reduces NO_3^- through a series of intermediates to N_2, and anammox, which forms N_2 by directly coupling NO_2^- with NH_4^+. Organisms responsible for denitrification and anammox proliferate in O_2 minimum zones (OMZs) of the modern oceans, which support 20–40% of global fixed N loss to the atmosphere[2].

Under the well-oxygenated modern atmosphere, OMZs ($O_2 < 20\,\mu mol\,l^{-1}$) comprise 7% by volume of the global ocean[3], and their anoxic cores, which sustain most fixed N loss, occupy only 0.1%[2]. During the Proterozoic eon, however, atmospheric O_2 levels were lower than today and vast regions of the ocean were anoxic[4]. Loss of fixed N is predicted under ocean anoxia and such expansive anoxia could have led to extreme N limitation[5]. N isotope distributions from Palaeoproterozoic upwelling systems, however, imply relatively little fixed N loss[6]. This suggests either modest rates of denitrification or N retention, possibly through reduction of NO_3^- to NH_4^+[6]. Notably, anoxia and a supply of NO_3^- will not support fixed N loss without electron donors to drive denitrification, or NH_4^+ to support anammox. In the modern ocean, denitrification is fuelled through both organic electron

donors and H_2S (refs 7,8). Organic electron donors may have been scarce under the generally low productivity of Proterozoic oceans[5], and H_2S would have been scarce except during episodic euxinic periods that punctuate the Proterozoic geologic record[6,9–12]. Ferruginous conditions were much more prevalent than euxinia, dominating ocean chemistry throughout the Proterozoic[13]. Ferrous Fe (Fe(II)) is known to support NO_3^- reduction in laboratory experiments[14,15] but the environmental operation, significance and pathways of Fe-dependent NO_3^- reduction remain untested in natural ferruginous water columns.

Kabuno Bay (KB) is a ferruginous sub-basin of Lake Kivu, which straddles the border of Rwanda and the Democratic Republic of Congo, East Africa[16]. Saline springs feed KB causing permanent stratification, anoxia below 10 m (Fig. 1a,b), and Fe(II)-rich deep waters ($\approx$500 μM—Fig. 1d). Such ferruginous conditions are analogous to those that prevailed through much of the Proterozoic eon[16]. A strong gradient of NH_4^+ between 10 and 11.5 m depth (Fig. 1c) indicates high rates of NH_4^+ oxidation to NO_3^- and NO_2^- within this depth interval. Since KB's oxic surface waters are devoid of NO_3^- and NO_2^- (concentrations <1 μM), NO_3^- and NO_2^- produced through NH_4^+ oxidation are advected to the main basin, assimilated, or rapidly reduced.

We determined rates and pathways of microbial N transformations in KB using incubations with ^{15}N-labelled NO_3^-. Both denitrification and dissimilatory nitrate reduction to ammonium (DNRA) occur between 11 and 11.5 m, but anammox was below

[1]Microbiology & Immunology, and Earth, Ocean, & Atmospheric Sciences Departments, University of British Columbia, Vancouver, BC V6T 1Z3, Canada. [2]Chemical Oceanography Unit, Université de Liège, 4000 Liège, Belgium. [3]Department of Earth & Environmental Sciences, KU Leuven, 3001 Leuven, Belgium. [4]Department of Genetics and Microbiology, Universitat Autònoma de Barcelona, 08193 Barcelona, Spain. [5]Institute of Life Sciences (ISV), Université Catholique de Louvain, 1348 Louvain-la-Neuve, Belgium. [6]Ecologie des Systèmes Aquatiques, Université Libre de Bruxelles, 1050 Bruxelles, Belgium. [7]Institute of Biology, Nordic Center for Earth Evolution, University of Southern Denmark, 5230 Odense, Denmark. [8]Research Unit in Environmental and Evolutionary Biology (URBE), University of Namur, 5000 Namur, Belgium. *e-mail: sean.crowe@ubc.ca
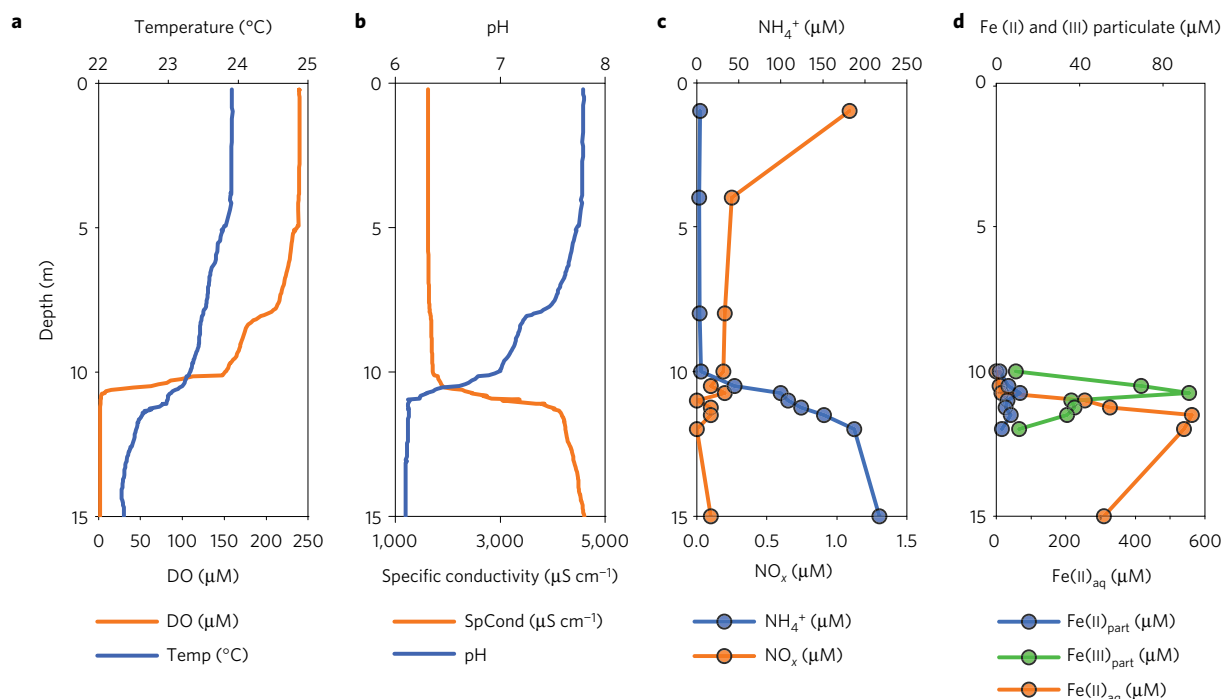
Figure 1 | Vertical distribution of selected physical and chemical properties of Kabuno Bay for February 2012. a, Dissolved O_2 (DO) concentration (μM) and temperature (°C). **b**, pH and specific conductivity (SpCond, $\mu S\ cm^{-1}$). **c**, NH_4^+ and NO_x concentration (μM). **d**, $Fe(II)_{aq}$, $Fe(II)_{part}$ and $Fe(III)_{part}$ concentrations (μM).

our limit of detection (6 nmol N l^{-1} d^{-1}). Rates of denitrification and DNRA were up to 80 ± 10 and 50 ± 10 nmol N l^{-1} d^{-1}, respectively (Fig. 2a,b and Supplementary Table 3), exceeding those typically found in marine OMZs[8,17] but similar to coastal marine anoxic basins such as the Baltic Sea[18]. While 60% of NO_3^- reduced is lost from the KB through denitrification, 40% is retained as NH_4^+ through DNRA. Substantial NO_3^- recycling to NH_4^+ has also been periodically observed in the Peruvian and Omani OMZs[17,19], but such a high fraction appears to be unusual for modern pelagic marine environments[8,20]. Our observations imply that some biogeochemical feature of KB favours DNRA compared with other environments studied to date. Fe(II), which is unusually abundant in KB, indeed promotes DNRA in estuarine sediments[21], and may also do so in KB.

To test for such Fe dependency, we amended a subset of our ^{15}N incubations with 40 μM Fe(II). We found that Fe(II) addition considerably enhanced both denitrification and DNRA to 230 ± 40 and 70 ± 20 nmol N l^{-1} d^{-1}, respectively (Fig. 2a,b and Supplementary Table 3), suggesting a role for Fe(II) in NO_3^- reduction. Our results support measurements from estuarine sediments, which invoke microbial mediation[21], but the nearly equivalent stimulation between both NO_3^- reduction to NH_4^+ and denitrification provides no evidence that Fe(II) favours DNRA and instead may indicate that Fe(II) enhances the reduction of an intermediate (for example, NO_2^-) common to both reactions. Thermodynamic considerations reveal that reduction of NO_3^-, and a number of intermediate N species, by Fe(II) is energetically favourable in KB (see Supplementary Information) yielding sufficient free energy for microbial growth. While the precise pathway remains unresolved, Fe(II) clearly plays a role in NO_3^- reduction in KB.

To assess the biogeochemical role of Fe-dependent NO_3^- reduction in KB, we compared rates of NO_3^- reduction with other key processes[16]. While Fe(II) supports NO_3^- reduction, the corresponding Fe(II) oxidation rates of 1,700 nmol Fe l^{-1} d^{-1} (based on stoichiometry) are only a minor fraction (1%) of the observed

phototrophic Fe(II) oxidation in the KB chemocline[16]. By comparison, NO_3^- reduction rates are an order of magnitude lower than SO_4^{2-} reduction rates, which are up to 410 nmol S l^{-1} d^{-1} (ref. 16). We also compared rates of NO_3^- reduction with dark carbon fixation, and on the basis of growth yields for chemoautotrophic NO_3^- reduction (see Supplementary Information), this comparison suggests that NO_3^--driven chemoautotrophy could support up to 2% of the total dark carbon fixation in KB's water column[16]. The overall contribution of NO_3^- reduction to biogeochemical cycling, therefore, is largely to regulate recycling and loss of fixed N from KB, and here, the partitioning of NO_3^- reduction between DNRA and denitrification is key.

We have shown that NO_3^- reduction both to N_2 and NH_4^+ takes place at relatively high rates under ferruginous conditions, and further, that this NO_3^- reduction is partly coupled to the oxidation of Fe(II). By extension, the ferruginous oceans of the Proterozoic eon could also have supported large-scale NO_3^- reduction, possibly through both denitrification and DNRA, and with Fe(II) as the electron donor[5,22]. To quantitatively link our observations in KB to possible biogeochemical cycling under ancient marine ferruginous conditions, we set up a box model for N cycling in ocean upwelling systems[23,24]. Our model describes mass balances for C, N, S, O and Fe species and their biogeochemical reactions (see Fig. 3a and full description in the Supplementary Information). NH_4^+ and Fe were supplied through upwelling, and these, along with nutrient recycling, ultimately controlled primary production in the overlying surface waters. Production in the surface waters is sustained exclusively through upwelled N with no productivity by local N fixation. Settling of organic matter generated through primary production drives respiration and nutrient recycling in intermediate waters. Chemotrophic processes such as nitrification, and Fe-dependent denitrification and DNRA were included (Fig. 3a). Our model is based on previous studies[23,24], but we considered a ferruginous system where N cycling was driven first by Fe-dependent NO_3^- reduction, with the remaining NO_3^- reduced by organic matter originating through primary production (Fig. 3a).
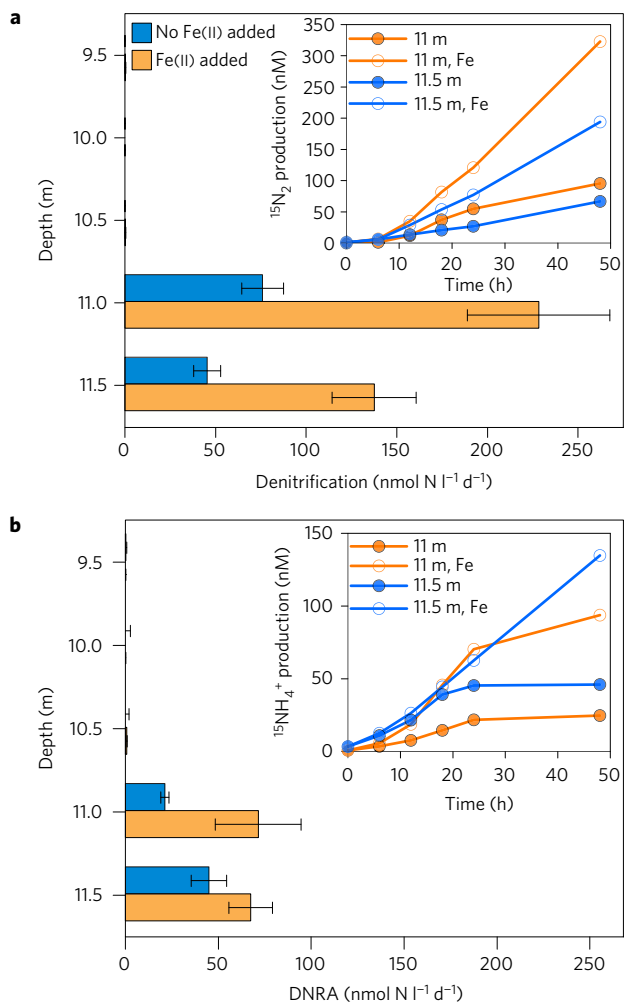
Figure 2 | Rates and pathways in Kabuno Bay for February 2012.
a,b, Denitrification (**a**) and DNRA (**b**) in Kabuno Bay water column. Samples were collected in February 2012, with (in orange) or without (in blue) addition of the electron donor Fe(II) to the incubations. Insets show time-course evolution of ^{15}N-labelled metabolic products. Rates were calculated on the basis of linear regressions over the linear data intervals (24 or 48 h). Supplementary Table 3 contains the detailed rates and associated errors. The error on the rate is the standard error of the slope for the linear regression.

We also included DNRA, in accordance with our results from KB, to evaluate its impact on coupled C, N, Fe and S cycling under ferruginous conditions. Without explicit constraints on the fraction of NO_3^- reduced to NH_4^+ versus N_2 in ferruginous oceans, we varied its contribution from 0 to 40%, with the balance occurring through denitrification.

Deep-ocean Fe(II) and NH_4^+ concentrations throughout the Proterozoic eon are uncertain. If global N fixation is limited by phosphorous supply according to the Redfield ratio (16N:1P; ref. 25), we can set deep-ocean NH_4^+ concentrations in our model at 16 times the phosphorous concentration (0.04–0.13 μM) of Proterozoic seawater[26] (see Supplementary Information), which yields up to 2 μM NH_4^+. To validate this assumption, we excluded DNRA and ran our model with different ratios of N/P in deep waters. When deep ocean NH_4^+ is greater than 13 μM, sulfidic conditions develop without DNRA or N fixation under all reasonable upwelling rates[23] (Fig. 3e). Thus, if deep-ocean NH_4^+ concentrations were more than 13 μM, sulfidic conditions would have been widespread during the Proterozoic eon. Such widespread

euxinia is not supported by the geologic record[13], indicating that NH_4^+ concentrations were generally less than 13 μM in the deep ocean. We thus chose 2 μM NH_4^+ as the benchmark for our modelling, but also explored a concentration range from 0.6 through to 13 μM. In line with considerations for both siderite solubility[27] and nutrient dynamics that permit marine oxygenic photosynthesis[26] we chose 42 μM as our benchmark Fe(II) concentration (see Supplementary Information). We also considered a broader range of Fe(II) concentrations (see Supplementary Information), which may be possible if siderite formation was kinetically inhibited[28].

Our model shows that in ferruginous upwelling systems the balance between DNRA and denitrification strongly influences coupled C, N, S and Fe cycling with enhanced primary production when DNRA is an appreciable NO_3^- reduction pathway. Indeed, when 40% of NO_3^- reduction is channelled through DNRA, primary production rates increase by up to 170% (Fig. 3b,c). A notable effect of this enhanced primary production is greatly increased H_2S production. This occurs even in the absence of N fixation as DNRA provides the nitrogen to stimulate additional organic matter production, which ultimately fuels microbial sulfate reduction (see Supplementary Information). At 40% DNRA, strong upwelling leads to sulfate reduction and pyrite deposition at rates sufficient to yield sediment iron speciation (Fe_{py}/Fe_{HR}) that indicates possible water column euxinia. Such Fe_{py}/Fe_{HR} values (>0.7) exist in Proterozoic sedimentary rocks[6,9–12], which could thus record a contribution of DNRA to NO_3^- reduction at this time.

Our model also reveals a negative feedback between primary production and surface ocean oxygen. This negative feedback develops when N loss increases in response to enhanced NO_3^- supply due to stimulation of nitrification by O_2. An increase from 3.8% to 6.2% PAL (present atmospheric level) O_2, values thought possible for the Mesoproterozoic[29] (values as low as 0.1% PAL have been proposed[30]), reduces primary production by up to 20% when NO_3^- reduction occurs exclusively through denitrification. This effect is muted by DNRA (Fig. 3b,c), which can play an increasingly important role in supplying N for primary production with the progressive oxygenation of the surface ocean (Fig. 3d).

It is widely assumed that the Proterozoic oceans were N limited due to massive N loss[5]. While the euphotic waters directly overlying upwelling systems can be locally N limited due to N loss from below, the global expression of N limitation ultimately depends on the balance between the geographic expansiveness of upwelling systems, and ocean-wide N fixation. We extrapolated N loss from our model to an area equivalent to upwelling regions in the modern ocean ($0.36 \, 10^{12} \, m^2$)[31] yielding a modelled global N loss from Proterozoic oceans of up to 1.6 Tg N yr^{-1} (see Supplementary Information). By comparison, Proterozoic phosphorous concentrations[26] could have supported 4.8 Tg of N fixation per year based on an equivalent ratio of N fixed to deep ocean phosphorous as in the modern ocean[25] (see Supplementary Information). It has also been proposed that molybdenum (Mo) limited N fixation due to its scavenging from seawater as sulfide minerals[32]. Mo limitation seems unlikely, as Mo scavenging from seawater generally requires strong euxinia (see Supplementary Information), which as we show here, would not likely have developed in Proterozoic upwelling systems. To balance global N fixation with N loss in the Proterozoic eon, an upwelling area three times that of the modern ocean would have been needed. This suggests that N limitation in the Proterozoic was unlikely and that productivity would, instead, have been limited by phosphorous. Our modelling results are well supported by the Palaeoproterozoic rock record[6], which implies upwelling systems with euxinic conditions (possibly supported by DNRA) that induce little fixed N loss (also possibly the result of DNRA). The operation of these processes throughout the Proterozoic eon can be further tested through an expansion of the N isotope record, and through simulations in global biogeochemical models informed by our data.
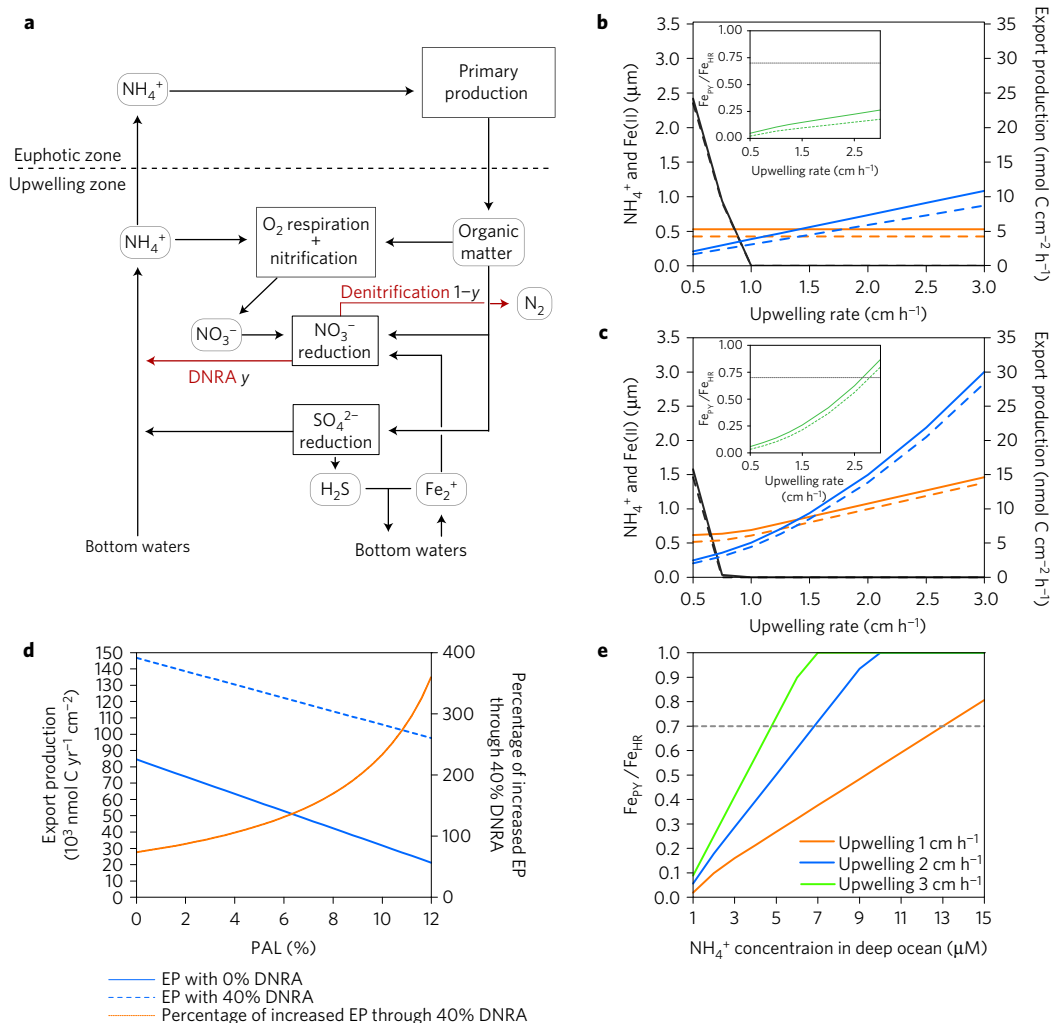
Figure 3 | Model outputs describing coupled C, N, S and Fe cycling in an idealized Proterozoic upwelling system. a, Model structure illustrating reactions included and their reactants and products. **b,c**, Model runs with 0% (**b**) and 40% NO_3^- reduction (**c**) through DNRA. The solid lines represent model runs with the surface water oxygen concentrations of 3.8% PAL, whereas the dashed lines represent runs at 6.2% PAL (blue, export production; orange, NH_4^+ concentrations in the upwelling zone; black, Fe(II) concentrations in the upwelling zone; the insets show the Fe pyrite to highly reactive Fe ratio (Fe_{PY}/Fe_{HR}) where the grey line delineates plausible euxinic conditions[13]). **d**, Yearly export production (EP) for 0% and 40% DNRA for a range of surface waters oxygen concentrations (from 0 to 12% PAL) at an upwelling rate of 2 cm h^{-1}. At 0% PAL, nitrification is not present in our model; however, NO_3^- is still supplied from the intermediate waters, therefore feeding NO_3^- reduction through DNRA and denitrification (see Supplementary Information). **e**, Fe_{PY}/Fe_{HR} ratios for a range of deep-ocean NH_4^+ concentrations at 0% DNRA for three different upwelling rates at 3.8% PAL (the grey dashed line delineates plausible euxinic conditions[13]). See Supplementary Information for details.

Methods

Methods, including statements of data availability and any associated accession codes and references, are available in the online version of this paper.

References

1. Vitousek, P. M. Human domination of Earth's ecosystems. *Science* **277,** 494–499 (1997).
2. Codispoti, L. A. *et al*. The oceanic fixed nitrogen and nitrous oxide budgets: Moving targets as we enter the anthropocene? *Sci. Mar.* **65,** 85–105 (2001).
3. Paulmier, A. & Ruiz-Pino, D. Oxygen minimum zones (OMZs) in the modern ocean. *Prog. Oceanogr.* **80,** 113–128 (2009).
4. Canfield, D. E. A new model for Proterozoic ocean chemistry. *Nature* **396,** 450–453 (1998).
5. Fennel, K., Follows, M. & Falkowski, P. G. The co-evolution of the nitrogen, carbon and oxygen cycles in the Proterozoic ocean. *Am. J. Sci.* **305,** 526–545 (2005).
6. Godfrey, L. V., Poulton, S. W., Bebout, G. E. & Fralick, P. W. Stability of the nitrogen cycle during development of sulfidic water in the redox-stratified late Paleoproterozoic Ocean. *Geology* **41,** 655–658 (2013).
7. Canfield, D. E. *et al*. A cryptic sulfur cycle in oxygen-minimum-zone waters off the Chilean coast. *Science* **330,** 1375–1378 (2010).
8. Kalvelage, T. *et al*. Nitrogen cycling driven by organic matter export in the South Pacific oxygen minimum zone. *Nat. Geosci.* **6,** 228–234 (2013).
9. Johnston, D. T. *et al*. An emerging picture of Neoproterozoic ocean chemistry: insights from the Chuar Group, Grand Canyon, USA. *Earth Planet. Sci. Lett.* **290,** 64–73 (2010).
10. Li, C. *et al*. A stratified redox model for the Ediacaran ocean. *Science* **328,** 80–83 (2010).
11. Poulton, S. W., Fralick, P. W. & Canfield, D. E. Spatial variability in oceanic redox structure 1.8 billion years ago. *Nat. Geosci.* **3,** 486–490 (2010).
12. Reinhard, C. T., Raiswell, R., Scott, C., Anbar, A. D. & Lyons, T. W. A late archean sulfidic sea stimulated by early oxidative weathering of the continents. *Science* **326,** 713–716 (2009).
13. Poulton, S. W. & Canfield, D. E. Ferruginous conditions: a dominant feature of the ocean through earth's history. *Elements* **7,** 107–112 (2011).
14. Straub, K. L., Benz, M., Schink, B. & Widdel, F. Anaerobic, nitrate-dependent microbial oxidation of ferrous iron. *Appl. Environ. Microbiol.* **62,** 1458–1460 (1996).

15. Weber, K. A., Urrutia, M. M., Churchill, P. F., Kukkadapu, R. K. & Roden, E. E. Anaerobic redox cycling of iron by freshwater sediment microorganisms. *Environ. Microbiol.* **8,** 100–113 (2006).

16. Lliros, M. *et al.* Pelagic photoferrotrophy and iron cycling in a modern ferruginous basin. *Sci. Rep.* **5,** 13803 (2015).

17. Lam, P. *et al.* Revising the nitrogen cycle in the Peruvian oxygen minimum zone. *Proc. Natl Acad. Sci. USA* **106,** 4752–4757 (2009).

18. Jensen, M. M., Petersen, J., Dalsgaard, T. & Thamdrup, B. Pathways, rates, and regulation of N_2 production in the chemocline of an anoxic basin, Mariager Fjord, Denmark. *Mar. Chem.* **113,** 102–113 (2009).

19. Jensen, M. M. *et al.* Intensive nitrogen loss over the Omani Shelf due to anammox coupled with dissimilatory nitrite reduction to ammonium. *ISME J.* **5,** 1660–1670 (2011).

20. De Brabandere, L. *et al.* Vertical partitioning of nitrogen-loss processes across the oxic-anoxic interface of an oceanic oxygen minimum zone. *Environ. Microbiol.* **16,** 3041–3054 (2014).

21. Robertson, E. K., Roberts, K. L., Burdorf, L. D. W., Cook, P. & Thamdrup, B. Dissimilatory nitrate reduction to ammonium coupled to Fe(II) oxidation in sediments of a periodically hypoxic estuary. *Limnol. Oceanogr.* **61,** 365–381 (2016).

22. Canfield, D. E., Rosing, M. T. & Bjerrum, C. Early anaerobic metabolisms. *Phil. Trans. R Soc. B* **361,** 1819–1834 (2006).

23. Canfield, D. E. Models of oxic respiration, denitrification and sulfate reduction in zones of coastal upwelling. *Geochim. Cosmochim. Acta* **70,** 5753–5765 (2006).

24. Boyle, R. A. *et al.* Nitrogen cycle feedbacks as a control on euxinia in the mid-Proterozoic ocean. *Nat. Commun.* **4** (2013).

25. Tyrrell, T. The relative influences of nitrogen and phosphorus on oceanic primary production. *Nature* **400,** 525–531 (1999).

26. Jones, C., Nomosatryo, S., Crowe, S. A., Bjerrum, C. J. & Canfield, D. E. Iron oxides, divalent cations, silica, and the early earth phosphorus crisis. *Geology* **43,** 135–138 (2015).

27. Holland, H. D. *The Chemical Evolution of the Atmosphere and Oceans* (Princeton Univ. Press, 1984).

28. Derry, L. A. Causes and consequences of mid-Proterozoic anoxia. *Geophys. Res. Lett.* **42,** 8538–8546 (2015).

29. Zhang, S. *et al.* Sufficient oxygen for animal respiration 1,400 million years ago. *Proc. Natl Acad. Sci. USA* **113,** 1731–1736 (2016).

30. Planavsky, N. J. *et al.* Low Mid-Proterozoic atmospheric oxygen levels and the delayed rise of animals. *Science* **346,** 635–638 (2014).

31. Martin, J. H., Knauer, G. A., Karl, D. M. & Broenkow, W. W. Vertex–carbon cycling in the northeast Pacific. *Deep-Sea Res.* **34,** 267–285 (1987).

32. Anbar, A. D. & Knoll, A. H. Proterozoic ocean chemistry and evolution: a bioinorganic bridge? *Science* **297,** 1137–1142 (2002).

Author contributions

F.D., A.V.B., C.C.M. and S.A.C. designed the experiments. F.D., F.A.E.R., S.A.C. and C.C.M. carried out the experiments. C.C.M. and S.A.C. analysed data and developed the model. C.C.M. and S.A.C. co-wrote the paper. All of the authors contributed to the revision of the paper.

Additional information

Supplementary information is available in the online version of the paper. Reprints and permissions information is available online at www.nature.com/reprints. Correspondence and requests for materials should be addressed to S.A.C.

Competing financial interests

The authors declare no competing financial interests.

Methods

Physico-chemical parameters as well as ^{15}N-labelled incubations were performed during a sampling expedition to Kabuno Bay (Lake Kivu, East Africa—1.58°–1.70° S, 29.01°–29.09° E) in February 2012. *In situ* vertical conductivity–temperature–depth (CTD) profiles were collected via two multi-parameter probes (Hydrolab DS5, OTT Hydromet; and Sea&Sun CTD90, Sea and Sun Technology). NO_2^- and NH_4^+ concentrations were measured spectrophotometrically[33]. Additionally, NO_3^- concentrations were determined by subtracting NO_2^- from the NO_x (NO_3^- and NO_2^-) measurements (via chemiluminescence[34]). Fe speciation was measured according to ref. 35. H_2S and SO_4^{2-} concentrations were determined using the Cline method[33] and ion chromatography (Dionex), respectively. ^{15}N-labelled incubations were performed in duplicate in 12 ml Exetainers, allowing water to be incubated under anoxic conditions. Microbial activity was arrested with $ZnCl_2$ at several time points for each experiment. The ^{15}N–N_2 and ^{15}N–NH_4^+ produced was quantified with isotopic ratio mass spectrometry. Rates of DNRA, denitrification and anammox were determined according to ref. 36. Rates were calculated on the basis of linear regressions with the least-squares method over the most linear data intervals (24 or 48 h). The structure of the box model set-up here is the same as that developed in ref. 23 and adapted for the Proterozoic eon in ref. 24. Details on model parameters can be found in the Supplementary Information.

Code availability. Our model was produced using Microsoft Office Excel. It is entirely reproducible using the information available in both the main text and the supplementary section.

Data availability. The authors declare that the data supporting the findings of this study are available within the article and its Supplementary Information files.

References

33. Grasshoff, K., Ehrhardt, M., Kremling, K. & Anderson, L. G. *Methods of Seawater Analysis* 3rd edn (Wiley, 1999).
34. Fontijn, A., Sabadell, A. J. & Ronco, R. J. Homogeneous chemiluminescent measurement of nitric oxide with ozone—implications for continuous selective monitoring of gaseous air pollutants. *Anal. Chem.* **42,** 575–579 (1970).
35. Viollier, E., Inglett, P. W., Hunter, K., Roychoudhury, A. N. & Van Cappellen, P. The ferrozine method revisited: Fe(II)/Fe(III) determination in natural waters. *Appl. Geochem.* **15,** 785–790 (2000).
36. Thamdrup, B. *et al*. Anaerobic ammonium oxidation in the oxygen-deficient waters off northern Chile. *Limnol. Oceanogr.* **51,** 2145–2156 (2006).